
Groundwater characterization of a heterogeneous granitic rock massif for shallow tunneling

J. FONT-CAPO^{|1,2|} E. VAZQUEZ-SUÑE^{|1|} J. CARRERA^{|1|} I. HERMS^{|3|}

^{|1|} Institute of Environmental Assessment and Water Research (IDAEA, CSIC)

C/ Jordi Girona, 18-26 08034 Barcelona Spain. Phone: +34 934 006 100 Fax: +34 932 045 904. Vazquez-Suñe E-mail: enric.vazquez@idaea.csic.es Carrera E-mail: jrcgeo@idaea.csic.es

^{|2|} Department of Geotechnical Engineering and Geosciences, Universitat Politècnica de Catalunya (UPC)-BarcelonaTech

C/ Jordi Girona, 1-3 Building D2 08034 Barcelona Spain. Phone: 93 401 72 50 Fax: 93 401 72 51

^{|3|} GEOCAT, Gestió de Projectes, S.A.

Av. Josep Tarradellas 34-36, 3a Floor 08029 Barcelona, Spain. Phone: +34 93 228 92 53 Fax: +34 93 425 20 01.
Herms E-mail: iherms@ggp.catgpp.cat

| A B S T R A C T |

Shallow tunneling may encounter a number of problems, the most important of which is high water inflows in transmissive areas that are often associated with fractures or discontinuities. Moreover, research into shallow tunneling may be limited by the duration and cost of the civil engineering works. Two important aspects that are often overlooked are: variable groundwater behavior of faults (conduit, barrier, conduit-barrier), and role of groundwater connectivity between fractures that cross the tunnel and the rest of the rock massif. These two aspects should be taken into account in the geological and groundwater characterization to correct the tunnel design and minimize hazards. A geological study and a preliminary hydrogeological characterization (including a prior steady state investigation and cross bore-hole tests) were carried out in a granitic sector during the construction of Line 9 of the Barcelona subway (B-20 area). The hydrogeological conceptual model was constructed using a quasi-3D numerical model, and different scenarios were calibrated. Faults and dikes show a conduit-barrier behavior, which partially compartmentalized the groundwater flow. The barrier behavior, which is the most marked effect, is more prominent in faults, whereas conduit behavior is more notable in dikes. The characterization of groundwater media entailed a dewatering plan and changes in the tunnel course. This enabled us to construct the tunnel without any problems.

KEYWORDS | Inflow. Shallow tunneling. Fault-zone. Modeling.

INTRODUCTION

Shallow tunneling may encounter a number of problems, the most important of which is high water inflows in transmissive areas that are often associated with fractures (Deva *et al.*, 1994; Tseng *et al.*, 2001; Shang *et al.*, 2004;

Dalgiç, 2003). Groundwater characterization is essential given that the association of soft materials and high water inflows may drag large amounts of material (Barton, 2000).

Groundwater in shallow tunneling is often approached in three steps. In the first step, attention is focused on con-

ductive areas that may represent groundwater inflows into the tunnel. These studies are usually undertaken by defining the major fractures or the most susceptible ones to produce tunnel inflows. In this regard, considerable research has been undertaken on a regional scale, *i.e.*, geological and geophysical studies, remote sensing and statistics have been employed to provide a rough idea of the most probable inflow areas (Banks *et al.*, 1992; Mabee *et al.*, 2002; Cesano *et al.*, 2000, 2003; Lipponen and Airo, 2006; Lipponen, 2007). In the second step, fractures are considered as transmissive inflow areas in order to locate and quantify tunnel inflows. This is calculated by analytical methods (Perrochet and Dematteis, 2007; Yang and Yeh, 2007) or by numerical methods (Molinero *et al.*, 2002; Yang *et al.*, 2009; Font-Capó *et al.*, 2011). The third step incorporates updated information into shallow tunneling, which enables us to predict future water inflows. However, these studies are often based on geomechanical and geological data of civil engineering works, which rarely take into account the hydraulic relationships with the rest of the rock massif (geological information is concentrated along the tunnel length, which is often paid little attention to).

From the standpoint of hydrogeology and tunneling, many authors consider that fractures and faults are areas with high permeability, preferential flow and conduit behavior (*e.g.*, Krisnamurthy *et al.*, 2000; Sener *et al.*, 2005; Shaban *et al.*, 2007; Mayer and Sharp, 1998; Flint *et al.*, 2001; Denny *et al.*, 2007; Cesano *et al.*, 2000, 2003; Mabee, 1999; Mabee *et al.*, 2002; Martinez-Landa and Carrera, 2005, 2006; Folch and Mas-Pla, 2008).

However, if the fractures are fault zones, they may act as localized conduits, barriers or conduit barriers, which are governed by commonly complex fault zone architecture and flow direction (Forster and Evans, 1991; Caine *et al.*, 1996; Caine and Forster, 1999; Caine and Tomusiak, 2003; Berg and Skan, 2005; Bense and Person, 2006). Fault-zones are conceptualized as fault cores surrounded by a damage zone, which differs structurally, mechanically and petrophysically from the undeformed host rock (protolith). The damage zone is usually considered as a higher permeability zone, whereas the core zone is regarded as a lower permeability zone. (Chester and Logan, 1986; Evans and Chester, 1995; Smith and Schwartz, 1984; Forster and Evans, 1991; Chester *et al.*, 1993; Bruhn *et al.*, 1994; Caine *et al.*, 1996; Evans *et al.*, 1997). Recent research has questioned the general applicability of this simple model (Faulkner *et al.*, 2010) for the following reason. Fault zones may contain a single fault core (sometimes with branching subsidiary faults) or a fault core that may branch, anatomize and link, entraining blocks or lenses of fractures and protolith between the layers, giving rise to asymmetric fault-zone areas (McGrath and Davison, 1995; Faulkner *et al.*, 2003; Kim *et al.*, 2004; Berg and Skar, 2005; Cembrano *et al.*, 2005; Cook *et al.*, 2006).

The structure of low and high permeability features can lead to extreme permeability heterogeneity and anisotropy (Faulkner *et al.*, 2010). The permeability of a fault zone in the plane and perpendicular to the plane (across-fault) is governed by the permeability of the individual fault rocks/fractures and more critically by their geometric architecture in three dimensions (Faulkner *et al.*, 2010; Lunn *et al.*, 2008). The capacity to form barriers to flow depends on the continuity of the low permeability layers (Faulkner and Rutter, 2001). The connectivity of the most permeable areas governs the permeability along and across the fault-zones (Faulkner *et al.*, 2010). The tunnel can cross fractures with a conduit, barrier or conduit-barrier behavior. The characteristics of crossed fractures determine the inflow volume that enters the tunnel.

Groundwater flow at a scale of the rock massif differs from that at fracture or fault scale. This factor is useful in tunneling. Several researchers have demonstrated that fluid-flow passes through few fractures in fractured massifs (Shapiro and Hsieh, 1991; Day-Lewis *et al.*, 2000; Knudby and Carrera, 2005; Martinez-Landa and Carrera, 2006). Increases in the volume of water flow depend on the continuity of well connected fractures (Knudby and Carrera, 2006). The effective transmissivity related to these fractures increases with scale (Illman and Neuman, 2001, 2003; Martinez-Landa and Carrera, 2005; Le Borgne *et al.*, 2006; Illman and Tartakowsky, 2006) or only in some particular directions (Illman, 2006). However, large scale permeability may decrease in massifs with a low permeability lineament network (Hsieh, 1998; Shapiro, 2003) where the fractures act as barriers that hinder connectivity and compartmentalize the flow (Bredehoeft *et al.*, 1992; Bense *et al.*, 2003; Bense and Person, 2006; Benedek *et al.*, 2009; Gleeson and Novakowski, 2009). The conduit-barrier behavior may also be expressed at a regional scale (Bense and Van Balen, 2004; Bense and Person, 2006; Bredehoeft *et al.*, 1992; Mayer *et al.*, 2007; Anderson and Bakker, 2008). The behavior of the fractures at a large scale plays a major role in tunneling. The water availability of the rocks and faults crossed by the tunnel is not only determined by their hydraulic characteristics but also by the connectivity with the boundary conditions and sources of water (Moon and Jeong, 2011).

The present paper addresses groundwater characterization of a fractured massif where shallow tunnels must be excavated. Characterization must be carried out at a scale that allows us to respond to the tunneling problems (design of the tunnel works, dewatering, inflows). The complex behavior of the faults and dikes, and the groundwater connectivity with the surrounding massif must be taken into account.

This characterization was implemented in the B-20 sector of Line 9 of the subway in Barcelona (Fig. 1A). In this area, the combination of intense fracturing and the presence of soft materials could give rise to problems in the tunneling works. A geological conceptual model was constructed, followed by a hydrogeological characterization. This model was validated by a quasi-3D numerical model that incorporated different scenarios of increasing complexity. Because of the time constraints of the project, only the conceptual model based on the geological and hydrogeological data was considered when implementing changes into the tunnel design and the dewatering plan. The numerical model and the simulations using different scenarios were carried out after the tunneling process.

GEOLOGICAL CONCEPTUAL MODEL

An accurate description of the structural geology at a large scale was first carried out. The main structures, lineaments, and geological changes that could constitute the

major flow conduits/pathways or barriers that may affect the groundwater were identified. A detailed geological study was undertaken after research at large scale. Where direct geological observation; (boreholes, outcrops...) were available, we could confirm the location of faults and dikes. In the B-20 area, the investigation was broadened to include a general characterization or large scale investigation (photogrammetry and geological interpretation of old aerial photographs) and detailed scale investigation; outcrop and borehole interpretation.

Accordingly, a large scale map showing the existence of granodiorite with numerous porphyritic dikes was made (Fig. 1B). Granodiorite is petrographically homogeneous. The porphyritic dikes, which are kilometers in length and meters wide, have a NE-SW trend and a sub-vertical dip, occurring in sub-parallel families. They can be observed and mapped only in outcrops outside the city centre. The dikes are more resistant to erosion than granodiorite, which facilitates identification. Subvertical strike-slip faults, trending NNW-SSE, separated by hundreds of meters

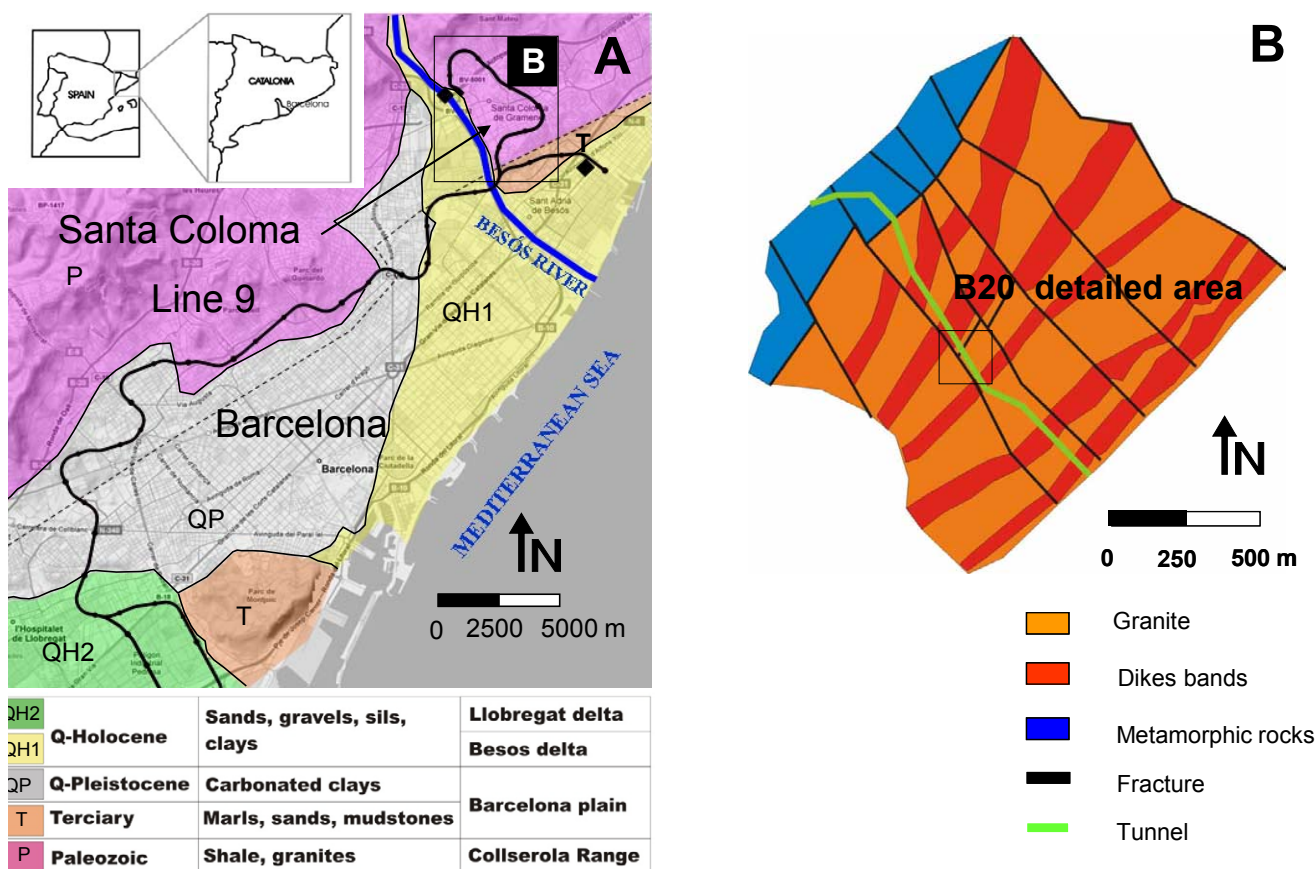


FIGURE 1 | A) Map of Barcelona conurbation and Line 9 subway. B) Large scale geological map of the Santa Coloma sector of Line 9 subway, B20 area.

displace the porphyritic dikes. These faults are late Carboniferous in age and affect Miocene sedimentary rocks south of the B-20 area, but they are absent in the B-20 area. This strongly suggests that they were reactivated in post-Miocene times (Martí *et al.*, 2008). In fact, the contact between granodiorites and Miocene sedimentary rocks is a normal fault zone similar to other normal faults that regionally generated the Miocene extensional basins related to the formation of the Catalan margin (Cabrera *et al.*, 2004). Cataclastic fault rocks (breccias and fault gouges) are usually associated with these normal faults.

A detailed geological investigation of the B-20 area was carried out using the borehole core interpretation in an attempt to improve the characterization of the granodiorite, granitic dikes, and fault-zones in this area (Fig. 2). The granodiorite rock unit may be divided into unaltered granite and weathered granite at a depth of 25–30 meters. Differences in the elevation of the unaltered granite-weathered granite contact on the two sides of structures 1 and 2 (Fig. 2) probably indicate that these lineaments are faults that separate two structural blocks. The dike area was divided into two NW-SE direction dikes on the basis of the information from the drilling cores.

HYDROGEOLOGICAL RESEARCH

Hydrogeological research was undertaken to define the fracture connectivity and hydraulic parameters of the rock massif units. This was carried out by studying hydrogeological features and by evaluating the hydraulic tests.

The piezometric level yielded indirect information about the relative relationships of the hydraulic parameters of the different formations. The piezometric heads can provide information about the contrast of hydraulic parameters between geological rock units and the lineament geometry. The presence of high hydraulic gradients may be associated with areas with groundwater flow obstacles (Bense and Person, 2006; Yechieli *et al.*, 2007; Gleeson and Novakoski, 2009; Benedek *et al.*, 2009).

A piezometric map of the area (Fig. 2) was made with the heads obtained in the drilling program. Heads display a high gradient along Fault 1 and Fault 2. The increase in gradient was attributed to a reduction in the transmissivity in the affected area. The presence of such areas in fractured massifs may be associated with low permeability fault zones that compartmentalize the flow. This barrier behavior may be ascribed at fracture scale to a reduction of the permeability in the central area of fault-zones (Evans, 1988; Goddard and Evans, 1995; Caine and Forster, 1999) or to the juxtaposition of different permeable layers due to fault movement (Bense *et al.*, 2003; Bense and Person, 2006).

The fractures or lineaments that play a significant role from a hydraulic point of view were identified. Hydraulic properties of these structures (conduit, barrier or conduit-barrier) must be characterized, which may be accomplished by hydraulic tests (Martinez-Landa and Carrera, 2006). Cross-hole tests, which have been used to characterize groundwater flow in fractured media, are instrumental in identifying connectivity and fracture extension (Guimera *et al.*, 1995; Day-Lewis *et al.*, 2000; Martinez-Landa and Carrera, 2006; Illman and Tartakowsky, 2006; le Borgne *et al.*, 2006; Benedek *et al.*, 2009; Illman *et al.*, 2009).

Six cross-hole tests were performed in the area (RSE Aplicaciones Territoriales SA, 2003). Five pumping wells and five piezometers were used. The wells and piezometers were screened in the two granite levels with the exception of Well 5 and the SC-17B piezometer, which were only screened in the shallow granite (Well 5 initially included the two granite layers but it was filled with concrete in order to test the shallow granite). All pumping tests were undertaken at a constant rate except pumping test 5, which was a step-drawdown test. Wells 1, 2, 3, 4 and 5 were used sequentially as pumping wells in the first five tests. Test number six was carried out by pumping simultaneously in three wells (Wells 1, 2, 3). Unfortunately, the drawdown responses were not measured in all the piezometers. Drawdown was measured in the following piezometers each of which corresponds to a pumping test: pumping test 1 (Wells 1, 2, 3, 4, 5, and piezometers SC-17B, SB20-3, SB20-5), pumping test 2 (Well 2 and piezometers SF28, SC-17B, and SB20-3), pumping test 3 (Wells 3, 4 and pi-

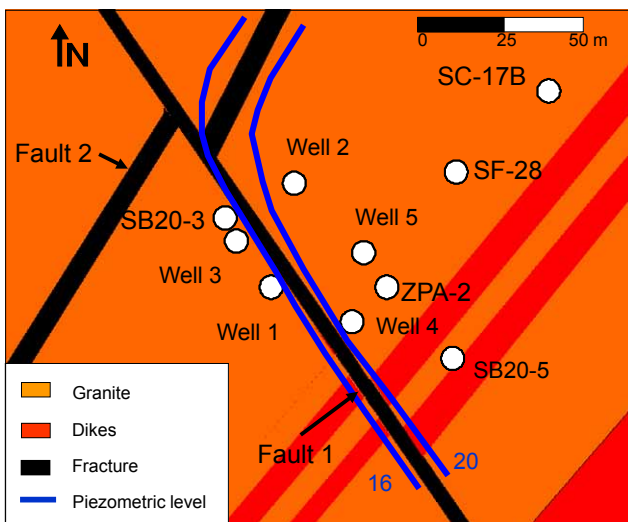


FIGURE 2 | Detailed scale geological map of the detailed area of B20, location of pumping wells and piezometers, and steady state piezometric surface.

ezometers SF-28, SC17-B, and SB20-3), pumping test 4 (Wells 2, 4 and piezometers SF-28, and SC-17B), pumping test 5 (Wells 1, 4, 5 and piezometers SF-28, ZPA-2, SC-17B, and SB20-5) and finally the triple pumping test (Wells 1, 2, 3, 4, 5 and SF-28, SC-17B and SB20-3). The wells and piezometers are shown in Figure 2.

A preliminary interpretation using analytical methods was made to analyze drawdowns, assuming that the medium is homogeneous and has an infinite extent. In these cross-hole tests, the drawdown curves were analyzed individually for each observation well in each pumping test. The transmissivity varied more than one order of magnitude, the pumping wells yielding lower transmissivities (50–250m²/d) than the piezometers (140 a 1800m²/d). The distribution of transmissivity values obtained from pumping wells does not allow distinguishing between the separate hydraulic formations and the better connected fractures. This can be achieved by storativity.

Storativity contains information and connectivity relationships. The estimated storativity is apparent and provides more information than the effective transmissivity values about the degree of connectivity between pumping and observation wells (Meier *et al.*, 1998; Sanchez-Vila *et al.*, 1999). Well connected points imply a rapid response to pumping. Rapid response can be estimated graphically by plotting drawdown versus the logarithm of time divided by the squared distance (log (t/r²)). If the medium was homogenous and isotropic, all the curves would be superimposed. A rapid response (in terms of t/r²) implies good connectivity. The value of t/r² used to determine the velocity of the response is the point t₀ where the line that joins the first drawdown points intersects the t/r² axis. The response of the different piezometers to pumping is plotted on the same graph (Fig. 3A). Drawdown was divided by the volume rate (s/Q) to eliminate the volume effect of each well in each pumping test. The results show differences of t₀ of five orders of magnitude, indicating a wide range of responses (Table 1). The most extreme piezometer responses are plotted in Figure 3B, C.

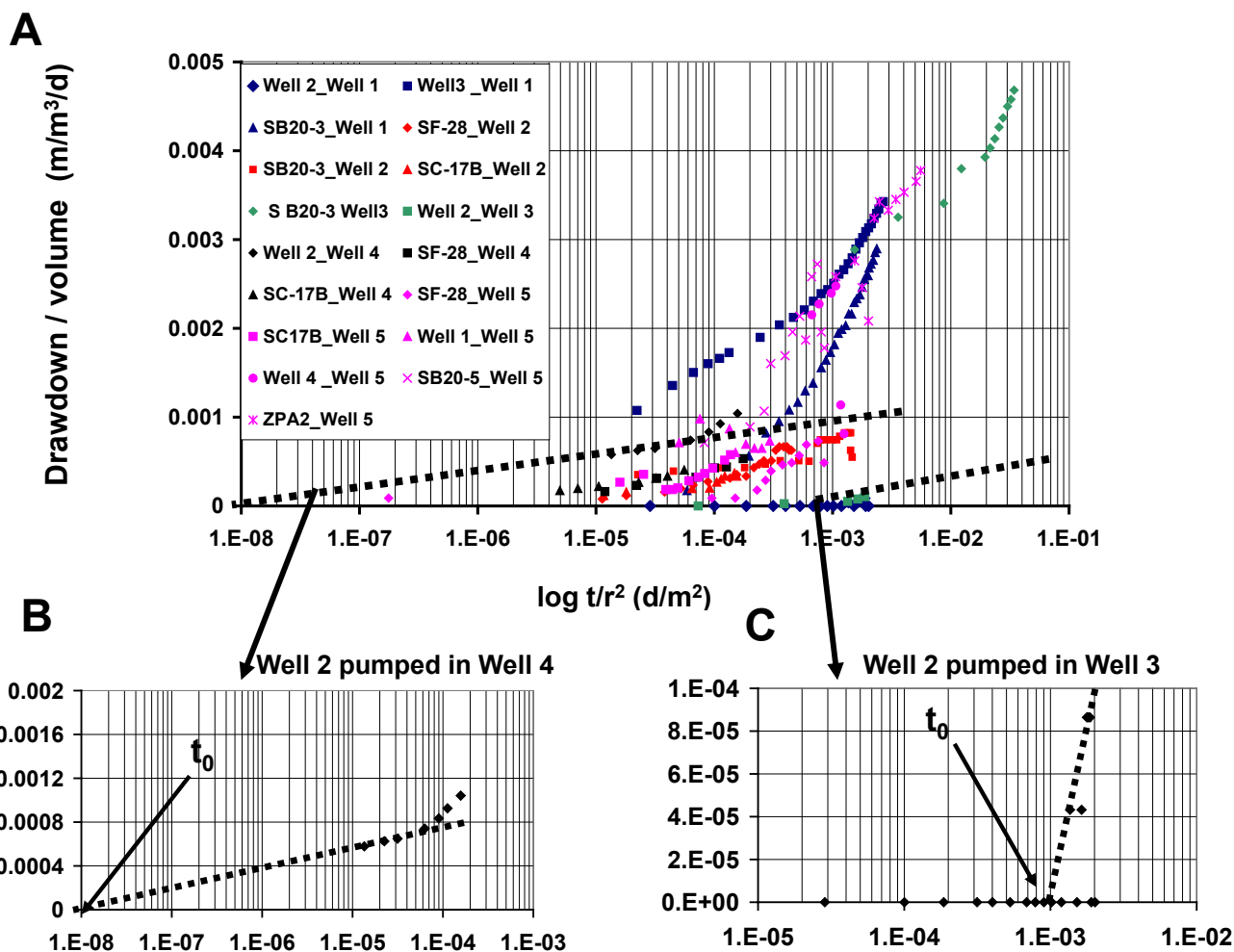


FIGURE 3 | A) Drawdown observed in the piezometers in response to the cross-hole tests. The time was divided by the squared distance between the pumping well and the piezometer, and the drawdown was divided by the pumped volume rate. B) The fastest (Well 2 pumped in Well 4) and the C) slowest (Well 4 pumped in Well 1) responses are plotted separately in order to show the detail of the methodology for each piezometer response.

TABLE 1 | Connectivity values of the observation wells (wells and piezometers) for the five pumping events

Observation well	Pumping well	t/r^2 (d/m ²)
Well 3	Well 1	1.0E-06
S20-03	Well 1	1.0E-04
Well 2	Well 1	1.0E-03
Well 4	Well 1	7.5E-03
Well 5	Well 1	no
S20-05	Well 1	1.0E-03
SC-17C	Well 1	no
SB20-03	Well 2	2.0E-09
SF-28	Well 2	7.0E-06
SC-17C	Well 2	7.0E-07
SB20-03	Well 3	1.0E-07
Well 2	Well 3	7.0E-05
SC-17C	Well 3	no
Well 2	Well 4	1.0E-08
SC-17C	Well 4	1.0E-07
S20-03	Well 4	no
SF-28	Well 4	4.0E-02
SC-17C	Well 5	5.0E-02
SF-28	Well 5	4.0E-02
S20-05	Well 5	1.0E-05
ZPA-2	Well 5	2.0E-04
Well 4	Well 5	2.0E-04
Well 1	Well 5	6.0E-03

The values of t/r^2 between pumping boreholes are plotted on the map (Fig. 4). The most prominent feature is the poor (or absence of) response between Wells 1 and 3 and the SB20-3 piezometer with respect to the rest of the modeled domain. The response between pumping Well 5 (weathered granite) and the rest of the piezometers shows medium-low values which could be due to the moderate connectivity value of the weathered granite. Well 2 has a moderate or high connectivity with Well 3 and piezometer SB20-3, respectively, which are located on the other side of the possible barrier structure that divides the domain. Lines of rapid response may be observed along the SC-17B - Well 4 axis and also between Wells 4 and 2.

DEFINITION OF THE GEOMETRICAL MODEL

The geometrical model was constructed using the above geological and hydrogeological results. The geological structures observed at large scale, basically the NNW-SSE trending faults and the SW-NE dike zones and faults) constitute the main discontinuities of the geometrical model. Only at detailed scale was it possible to combine the results of the geological and hydrogeological research. Fault 1 presented four important characteristics: a fault-zone de-

tected in large scale geological studies, a jump in depth of the contact between weathered-unaltered granite granodiorite across the fault, a high hydraulic gradient, and a poor cross-hole test response between the wells on both sides of the surface of the discontinuity. Despite the fact that fault 2 had similar geometrical characteristics, the hydraulic gradient was less marked and the bore hole test did not include information about this structure. These two faults were included as fractures in the conceptual model. In the case of dikes, a preferential connectivity direction was observed along the dike axis between piezometers SC-17B and Well 4. Furthermore, the contact between the dike and granite usually involves an increase in water volume extraction in the drilling process of the boreholes. This prompted us to include a longitudinal band of fractured zones along the less permeable dike axis. Double banded structures with conduit-barrier behavior exist in some dike-granitic areas (Gudmundson, 2000; Babiker and Gudmundson, 2004; Sultan, 2008). Intermediate connectivity between Well 5 (weathered granite) and the piezometers located in dike areas suggest a medium connectivity in the upper layer. Good connectivity between Wells 2 and 4 would imply the existence of a transmissive band of fractured rocks along the low permeable fault core in fault 1. Faults 1 and 2 were therefore transformed into a conduit-barrier system. All these geological and hydrogeological constraints were incorporated into the different models in order to test their validity.

NUMERICAL MODEL

The aim of the numerical model is twofold: quantify the hydraulic parameters of the different lithologies of the rock massif taking into account the main hydraulic geological features and calibrate the geometrical model

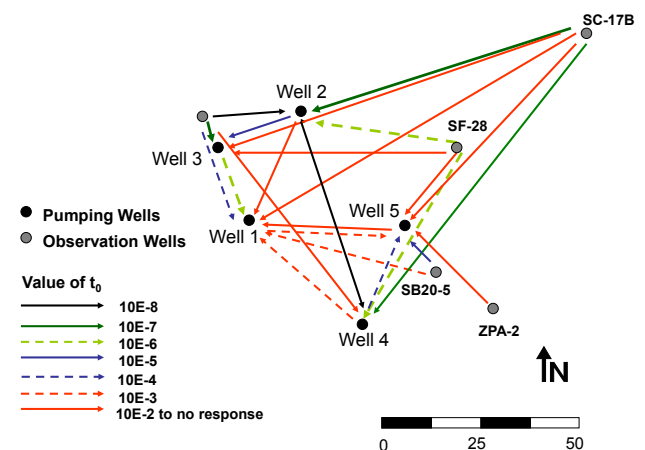


FIGURE 4 | Connectivity relationships between wells and piezometers in Figure 3 are represented geographically. Each order of magnitude of t/r^2 is plotted in a different color. Scale bar in meters.

verifying the hydraulic effect of the incorporated geological structures.

The numerical model was built after determining the main geological structures and defining the geometrical conceptual model. The model was constructed using a mixed discrete-continuum approach in line with the methodology of Martínez-Landa and Carrera (2006). The model treated the main geological structures (faults and dikes) separately from the rest of the rock matrix (granodiorite). A quasi-3D model (two layers) was constructed to differentiate the lower layer of unaltered granite from the surface layer of weathered granite.

The numerical model was performed with the finite element code VisualTRANSIN (Grupo de Hidrología Subterránea, 2003; Medina and Carrera, 1996). The model was limited by no flow boundaries (Fig. 5), that were chosen to lie on structure zones along the NW and SE margins and fault-zones along the SW and NE margins. Faults and dikes were detected in the two layers and were simulated as vertical structures for the sake of simplicity. The six pumping tests were calibrated in drawdown mode simultaneously, by simulating them on one run where the beginning of each test is marked by setting a zero drawdown at all model nodes activating the flow rate at the pumping well. The method required specifying standard deviations for model and measurement errors. These were higher in pumping wells (4-10m) than in piezometers (0.01-0.2m) because part of the pumping well drawdown was attributed to well loss and skin effects that were not modeled. Figures 6 and 7 do not show the drawdown of all the wells and piezometers since it was not possible to measure drawdowns at all observation wells. Drawdowns of the pumping wells are not illustrated in these figures because their weight was negligible in the calibration process.

Four scenarios, which increased in complexity from the homogeneous model to the geometrical model defined above (Fig. 8), were calibrated in order to obtain the most suitable solution: a homogeneous model; a barrier fault model (differentiating the characteristics of granite on both sides of fault 1); a barrier model for faults and dikes; and a conduit-barrier model constructed with the damage zones surrounding the faults and the transmissive areas along the dike axes.

RESULTS

The first scenario (homogeneous medium) yielded a poor fit at all piezometers (Figs. 6; 7). The poor fit was especially noticeable when it corresponded to the pumping wells located on the other side of the axis of fault 1 (not

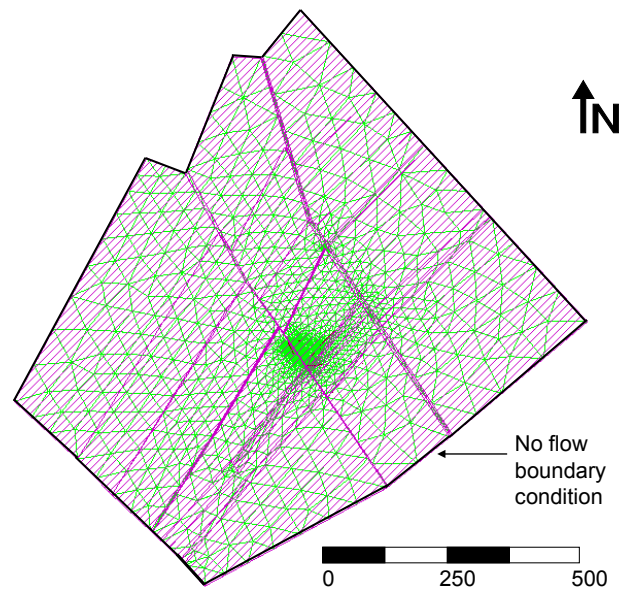


FIGURE 5 | Boundaries and finite element mesh of the numerical model and detailed B20 area. Faults and dikes have a finer discretization. Scale bar in meters.

active in this scenario). That is, the SB20-03 piezometer and Wells 1 and 3 produced a poor response to the pumping of wells 2, 4 and 5, as did the SC-17B, ZPA-2, SF-28 piezometers to Wells 1 and 3 (piezometer SB20-3 in the Fig. 7).

The second scenario incorporated the faults (barrier effect) and the differences in the transmissivity of the granites on both sides of Fault 1 (Fig. 6). This scenario simulated the barrier effect better because of Fault 1, which entailed a reduction in calculated drawdown of the piezometers that responded to the pumping wells located on the other side of fault 1. The piezometers located on the south-western side of fault 1 (wells 1 and 3, and the SB20-3 piezometer) yielded a good fit with respect to the pumping on the same side of the fault.

The third scenario introduced the SW-NE trending dikes into the model geometry. There was a notable improvement in some piezometers (ZPA-2). However, the fit was equal to, or worse than, that of the second scenario in the other piezometers. Calculated drawdown was higher than observed in the majority of the piezometers (Fig. 6). This problem was resolved and tested in the fourth scenario by implementing high transmissivity bands surrounding the faults and the dikes (conduit-barrier model). This yielded a better fit, resulting in a decrease in calculated drawdown. The transmissive bands dikes and faults between the SB20-5 piezometer and the pumping wells gave rise to flow paths, yielding a good fit (Fig. 7).

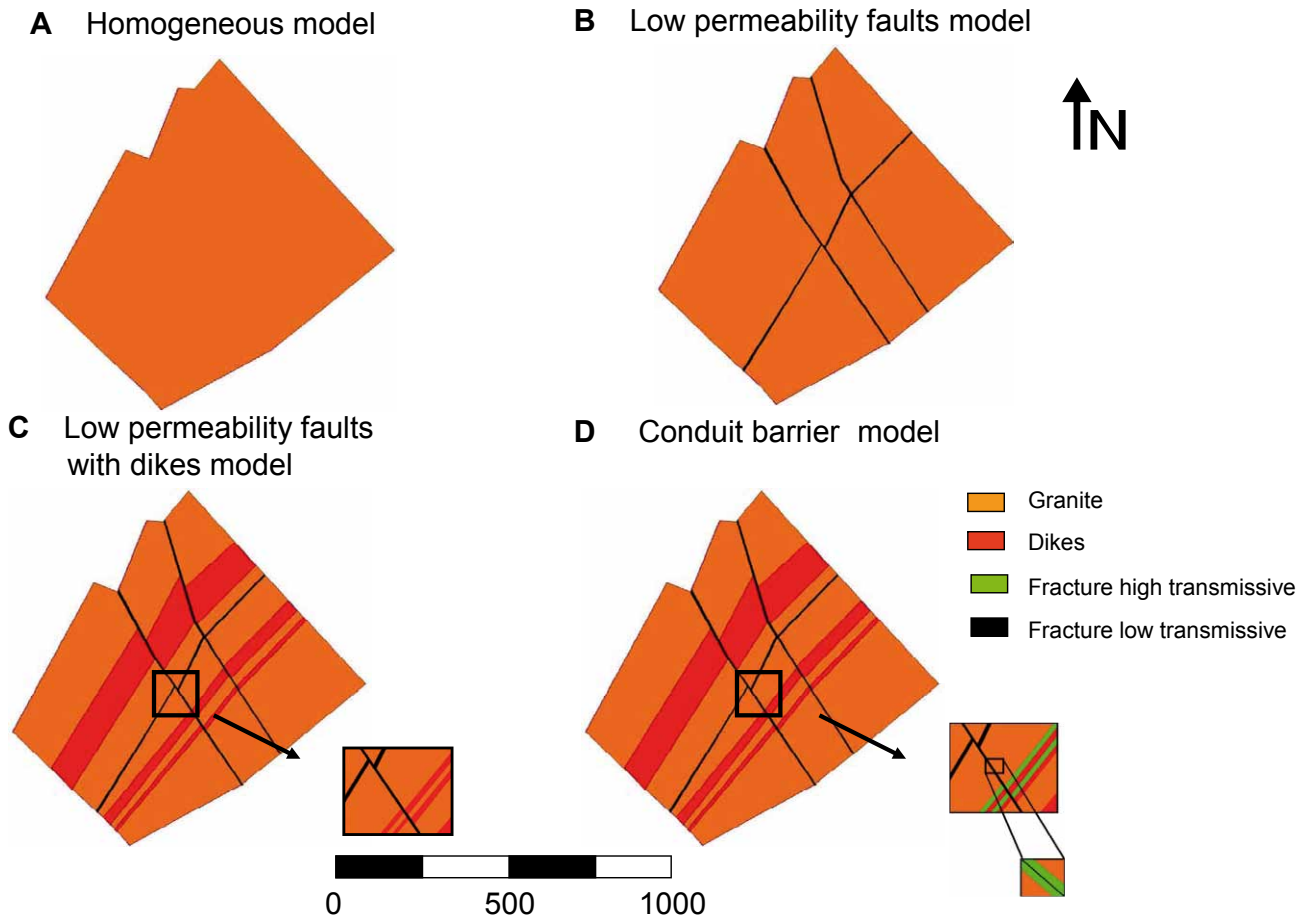


FIGURE 6 | Four scenarios calibrated in the numerical model. A) Homogeneous model B) Low permeability faults model C) Low permeability faults with dikes model D) Conduit barrier model. Scale bar in meters.

The fit in the SF-28 (Fig. 7) and SC-17B piezometers was always poor for pumping Well 2. Good connectivity between SB20-3 and Well 3 with Well 2 could be ascribed to the influence of Fault 2 (there is less hydrogeological information about fault 2 than about Fault 1), which enhances the flow across Fault 1 in this area (Figs. 4; 6; 7). And finally there is non symmetric behavior between Wells 1 and 5. Well 1 yields a better response to the pumping of well 5 than Well 5 to the pumping of Well 1. This behavior could be attributed to the differential drawdown caused by each well depending on the transmissivity of the affected area. When a well is located in a high transmissivity area or when it has well connected pathways, drawdown may be transmitted a considerable distance, possibly lowering heads below some transmissive fractures. By contrast, if the area surrounding the well has less transmissivity, the well will not be able to transmit drawdown very far. In consequence, the behavior between two boreholes does not have to be symmetrical. Our model was not able to simulate this behavior prob-

ably because of the addition of concrete in Well 5 to seal the lower granite.

In summary, the model was very sensitive to the barrier structures, especially the fault-zones. The definition of Fault 1 as a barrier was crucial for explaining the response to the pumping on the other side of the fault. The presence of the dike fractured bands (high and low permeability) and the high transmissivity areas surrounding the faults enabled us to reduce drawdown and to obtain the best fit in the northern block. The hydraulic parameters of the geological rock units are shown in Table 2. The transmissivity values of the weathered granite are very similar to those of the unaltered granite despite the fact that we expected them to be higher. We attribute this apparent contradiction to the intense fracturing of the upper portion of the unaltered granite. Furthermore, the fact that the wells and piezometers were mainly screened in the two granite layers hampered the separation of the parameters of the two layers.

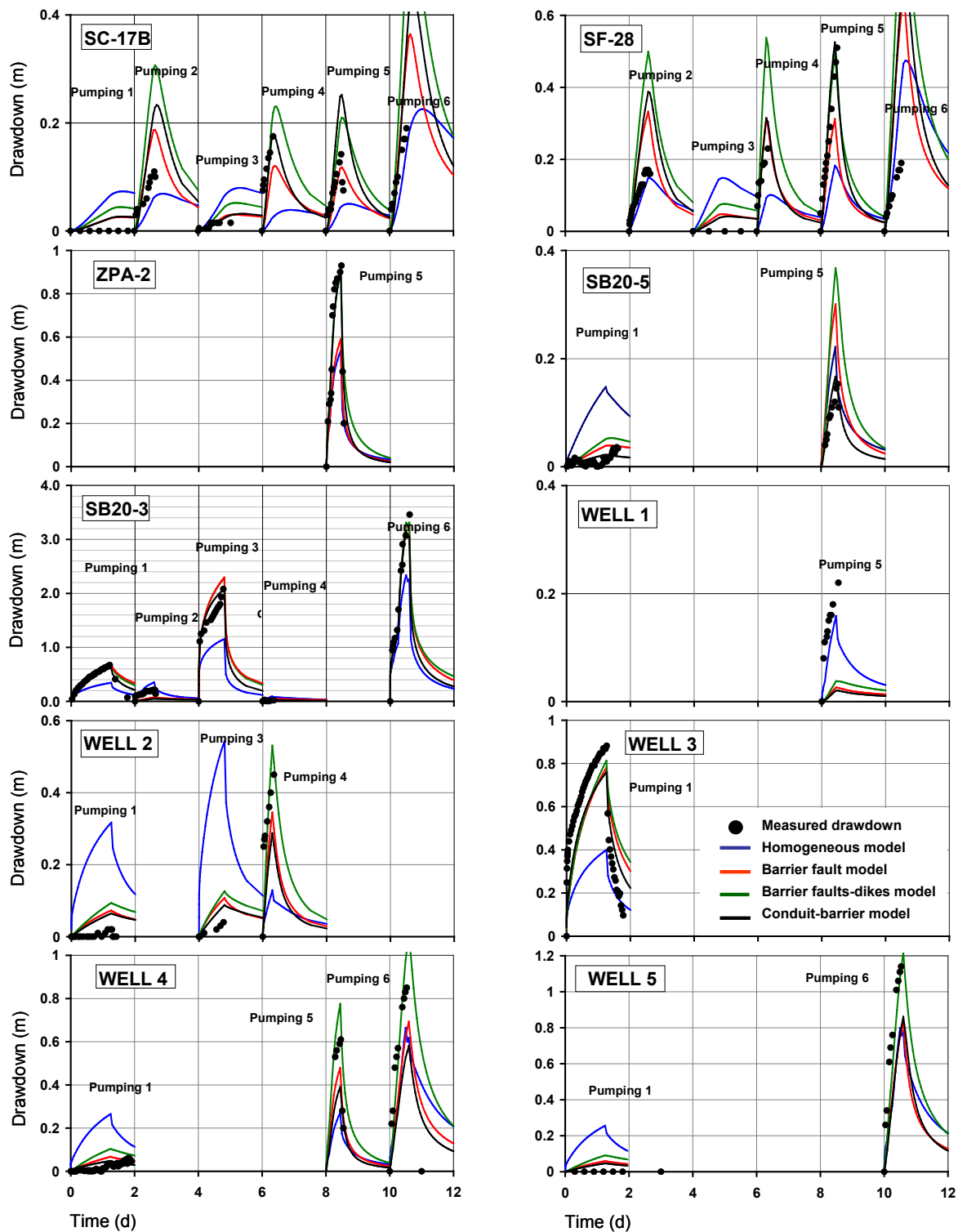


FIGURE 7 | Drawdown fits of the four calibrated scenarios for the five piezometers and pumping wells. The six pumping tests are calibrated consecutively with intervals of five days, returning to the 0 level of drawdown five days after to start the pumping test.

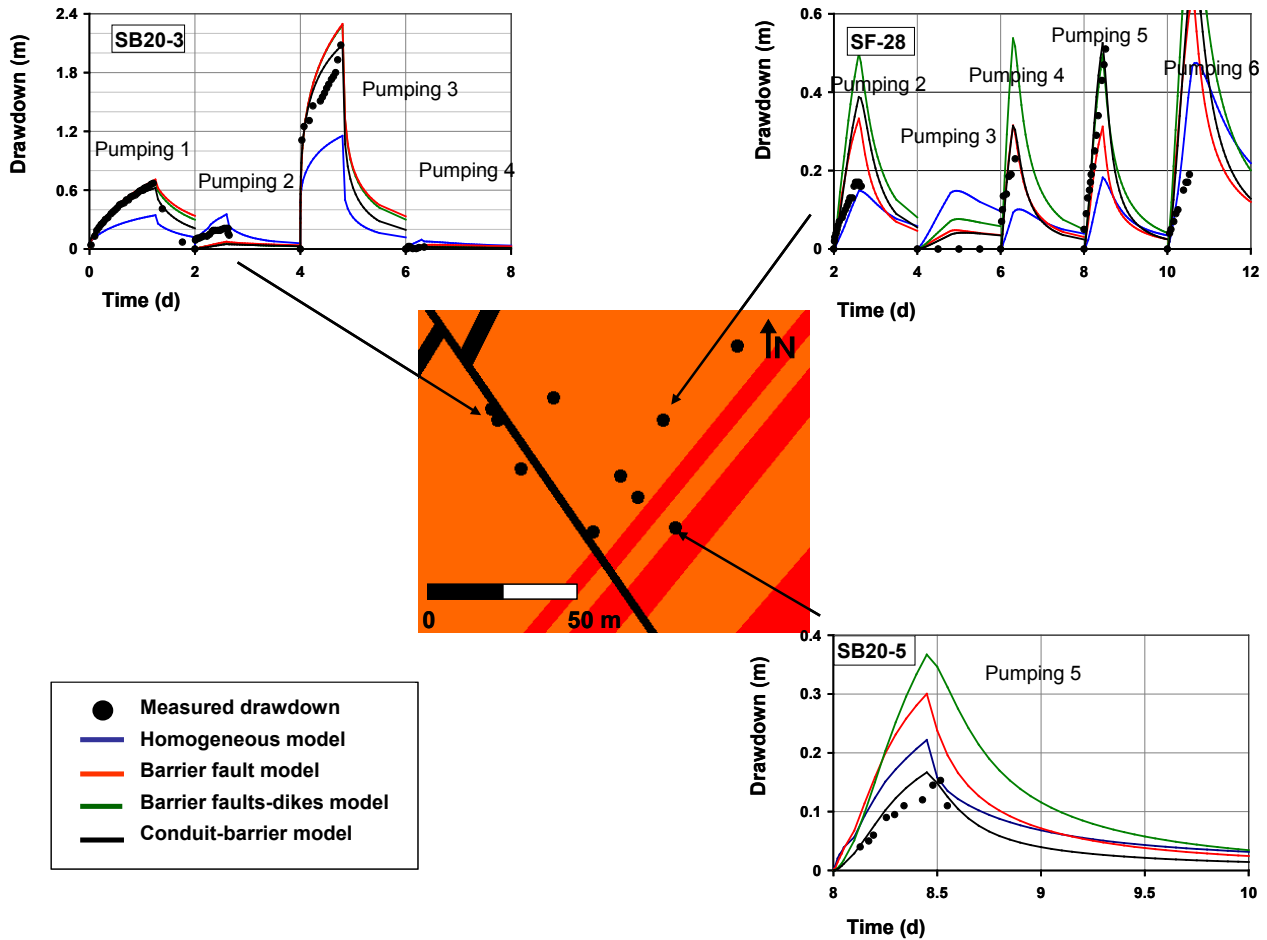


FIGURE 8 | Drawdown fits of the four calibrated scenarios for the three most representative piezometers, SF-28, SB20-3 and SB20-5.

DISCUSSION AND CONCLUSIONS

Groundwater characterization of a fractured massif of shallow tunneling was undertaken successfully. Geological characterization and groundwater research played a major role in building a conceptual model that reflected the groundwater flow in a fractured rock massif. Numerical modeling enabled us to test the reliability of the original hypotheses.

The complex groundwater behavior of the fractures was characterized in the B-20 area. Cross-hole tests proved crucial for characterizing the connectivity between the faults and dikes and granodiorite. The fault-zones provided evidence of a conduit-barrier behavior. The barrier effect was more marked than the conduit effect in faults, resulting in a groundwater behavior in blocks. The conduit effect was more prominent than the barrier effect in dikes. The most transmissible areas were those located along the contact of dikes and granite. The

area that was not covered by the cross-hole test mesh presented some problems of definition. Connectivity between well 2 and the other side of Fault 1 is not well represented in the model since Fault 2 is very close to this lineament. The absence of piezometers on the other side of this fault made its characterization difficult. The fact that the research was not restricted to the tunnel pathway enabled us to characterize the flow connectivity between the tunnel area and the rest of the rock massif. The exten-

TABLE 2 | Transmissivity values of the geological formations calibrated in the conduit barrier model

Rock unit	Transmissivity m^2/d
Weathered granite	20-30
Granite	20-50
Damage bands	600-5000
Core fault	0.1-0.2
Core dike	0.1-1

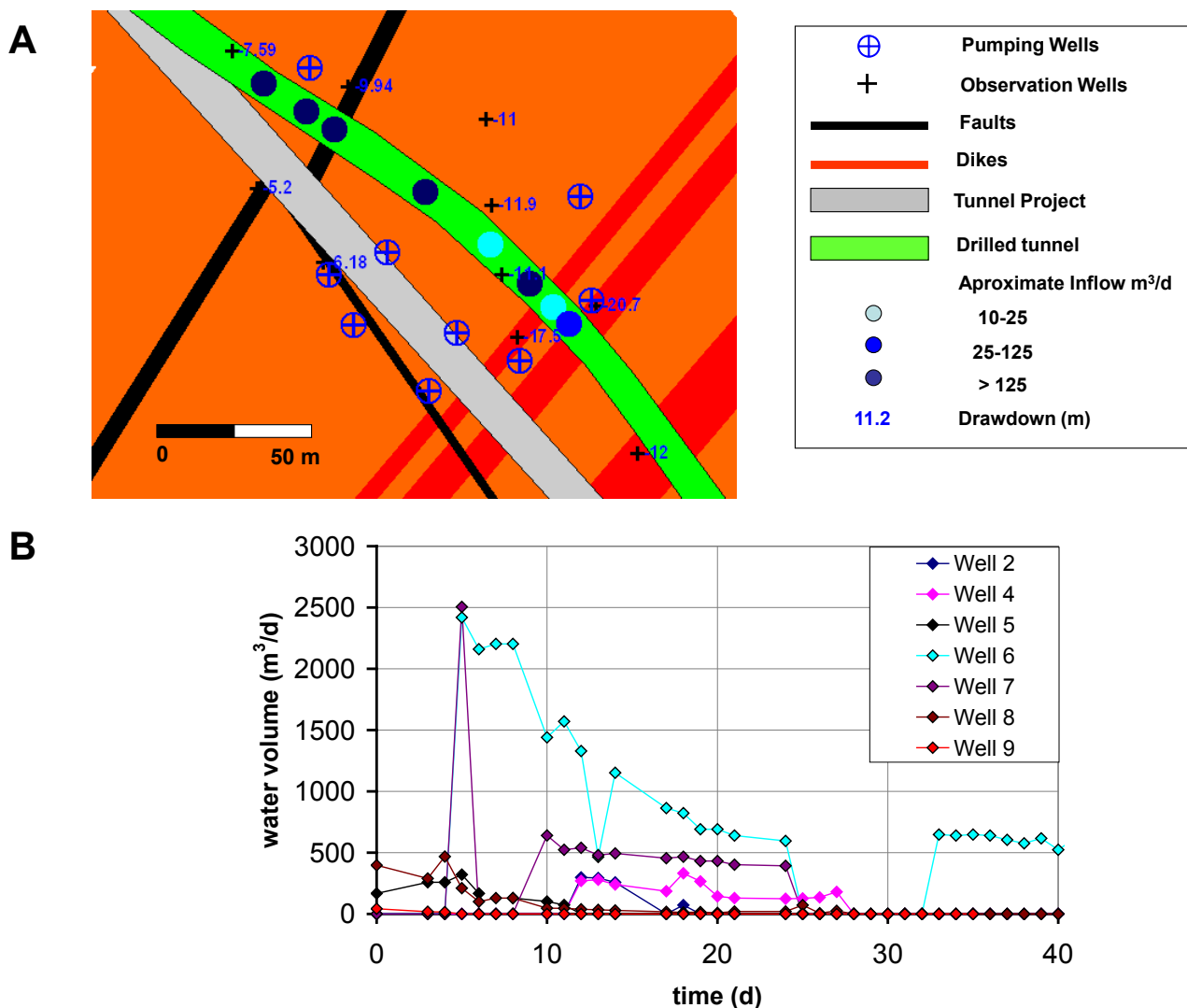


FIGURE 9 | A) Detailed area map with the location of the dewatering wells, piezometers (with their medium drawdown during the dewatering), and approximate tunnel inflow. B) Volume rate of the pumping wells during the dewatering event.

sion of the barrier and the conduit structures determined the flow in the tunnel area.

The barrier behavior was instrumental in dewatering because it compartmentalized the flow and reduced the pumped volume and water inflows. The general drawdown of the area (tunnel inflow+dewatering) is illustrated in Figure 9A, which shows that groundwater is compartmentalized and that the piezometers on the south side of fault 1 have a lower drawdown. The most volumetric dewatering boreholes (Wells 6 and 7, Fig. 9B) were located in the dike areas, especially in the more transmissive bands (Fig. 9A). Higher tunnel inflows (qualitative information) were located before fault 2 and in the dike area (Fig. 9A). A point of high water

inflow was located near Well 2, which could be due to the fact that Fault 2 was imperfectly defined.

ACKNOWLEDGMENTS

This work was funded by GISA Gestió d'Infraestructures S.A. (Generalitat de Catalunya). Other financial support was provided by the Spanish Ministry of Science and Innovation (HEROS project: CGL2007-66748 and MEPONE project: BIA2010-20244); Spanish Ministry of Industry (GEO-3D Project: PROFIT 2007-2009; and the Generalitat de Catalunya (Grup Consolidat de Recerca: Grup d'Hidrologia Subterrània, 2009-SGR-1057). We would like to thank Dr. F.J. Elorza and Dr. J. Escuder-Viruete for their comments on the manuscript that have helped to improve the revised version of the paper.

REFERENCES

- Anderson, E.I., Bakker, M., 2008. Groundwater flow through anisotropic fault zones in multiaquifer systems. *Water Resources Research*, 44(1-11).
- Babiker, M., Gudmundsson, A., 2004. The effects of dykes and faults on groundwater flow in an arid land: the Red Sea Hills, Sudan. *Journal of Hydrology*, 297(1-4), 256-273.
- Banks, D., Solbjorg, M., Rohrtorp, E., 1992. Permeability of fracture-zones in a precambrian granite. *Quarterly Journal of Engineering Geology*, 25(4), 377-388.
- Barton, N., 2000. TBM tunnelling in jointed and faulted rock. Rotterdam, Balkema, 172 pp.
- Benedek, K., Bothi, Z., Mezo, G., Molnar, P., 2009. Compartmented flow at the Bataapati site in Hungary. *Hydrogeology Journal*, 17(5), 1219-1232.
- Bense, V., Person, M., 2006. Faults as conduit-barrier systems to fluid flow in siliciclastic sedimentary aquifers. *Water Resources Research*, 42(5), W05421 (1-18).
- Bense, V., Van Balen, R., 2004. The effect of fault relay and clay smearing on groundwater flow patterns in the lower Rhine Embayment. *Basin Research*, 16(3), 397-411.
- Bense, V., Van Balen, R., de Vries, J., 2003. The impact of faults on the hydrogeological conditions in the Roer Valley rift system: an overview. *Netherlands Journal of Geosciences-Geologie en Mijnbouw*, 82(1), 41-54.
- Berg, S., Skar, T., 2005. Controls on damage zone asymmetry of a normal fault zone: outcrop analyses of a segment of the Moab fault, SE Utah. *Journal of Structural Geology*, 27(10), 1803-1822.
- Bredhoeft, J., Belitz, K., Sharphansen, S., 1992. The hydrodynamics of the big horn basin - a study of the role of faults. *Bulletin-American Association of Petroleum Geologists (AAPG)*, 76(4), 530-546.
- Bruhn, R., Parry, W., Yonkee, W., Thompson, T., 1994. Fracturing and hydrothermal alteration in normal-fault zones, *Pure and Applied Geophysics*, 142(3-4), 609-644.
- Cabrera, L., Roca, E., Garcés, M., de Porta, J., 2004. Estratigrafía y evolución tectosedimentaria oligocena superior-neógena del sector central del margen catalán (Cadena Costero-Catalana). In: Vera, J.A. (ed.). *Geología de España*. Sociedad Geológica de España, Instituto Geológico y Minero de España (IGME), 569-573.
- Caine, J., Evans, J., Forster, C., 1996. Fault zone architecture and permeability structure. *Geology*, 24(11), 1025-1028.
- Caine, J., Forster, C., 1999. Fault zone architecture and fluid flow: Insights from field data and numerical modeling. In: Mozley, P.S., Moore, J.C., Haneberg, W.C., Goodwin, L.B. (eds.). *Faults and subsurface fluid flow in the shallow crust*. American Geophysical Union geophysical monograph, 113, 101-127.
- Caine, J., Tomusiak, S., 2003. Brittle structures and their role in controlling porosity and permeability in a complex Precambrian crystalline-rock aquifer system in the Colorado Rocky Mountain Front Range. *Geological Society of America*, 115(11), 1410-1424.
- Cembrano, J., González, G., Arancibia, G., Ahumada, I., Olivares, V., Herrera, V., 2005. Fault zone development and strain partitioning in an extensional strike-slip duplex: A case study from the Mesozoic Atacama fault system, Northern Chile. *Tectonophysics*, 400(1-4), 105-125.
- Cesano, D., Bagtzoglou, A., Olofsson, B., 2003. Quantifying fractured rock hydraulic heterogeneity and groundwater inflow prediction in underground excavations: the heterogeneity index. *Tunnelling and Underground Space Technology*, 18(1), 19-34.
- Cesano, D., Olofsson, B., Bagtzoglou, A., 2000. Parameters regulating groundwater inflows into hard rock tunnels - a statistical study of the Bolmen tunnel in southern Sweden. *Tunnelling and Underground Space Technology*, 15(2), 153-165.
- Chester, F., Logan, J., 1986. Implications for mechanical-properties of brittle faults from observations of the punchbowl fault zone, California. *Pure and Applied Geophysics*, 124(1-2), 79-106.
- Chester, F., Evans, J., Biegel, R., 1993. Internal structure and weakening mechanisms of the San-Andreas fault. *Journal of Geophysical Research-Solid Earth*, 98(B1), 771-786.
- Cook, J.E., Dunne, W.M., Onasch, C.A., 2006. Development of a dilatant damage zone along a thrust relay in a low-porosity quartz arenite. *Journal of Structural Geology*, 28(5), 776-792.
- Dalgıç, S., 2003. Tunneling in fault zones, Tuzla tunnel, Turkey. *Tunnelling and Underground Space Technology*, 18(5), 453-465.
- Day-Lewis, F., Hsieh, P., Gorelick, S., 2000. Identifying fracture-zone geometry using simulated annealing and hydraulic-connection data. *Water Resources Research*, 36(7), 1707-1721.
- Denny, S.C., Allen, D.M., Journeay, J.M., 2007. DRASTIC-FM: a modified vulnerability mapping method for structurally controlled aquifers in the southern gulf Islands, British Columbia, Canada. *Hydrogeology Journal*, 15(3), 483-493.
- Deva, Y., Dayal, H., Mehrotra, A., 1994. Artesian blowout in a tbn driven water conductor tunnel in northwest Himalaya, India. In: *Proceedings 7th International IAEG Congress*, 4347-4354.
- Evans, J., 1988. Deformation mechanisms in granitic-rocks at shallow crustal levels. *Journal of Structural Geology*, 10(5), 437-443.
- Evans, J., Chester, F., 1995. Fluid-rock interaction in faults of the San-Andreas system - inferences from San-Gabriel fault rock geochemistry and microstructures. *Journal of Geophysical Research-Solid Earth*, 100(B7), 13007-13020.
- Evans, J., Forster, C., Goddard, J., 1997. Permeability of fault-related rocks, and implications for hydraulic structure of fault zones. *Journal of Structural Geology*, 19(11), 1393-1404.
- Faulkner, D., Lewis, A., Rutter, E., 2003. On the internal structure and mechanics of large strike-slip fault zones: field observations of the Carboneras fault in southeastern Spain. *Tectonophysics*, 367(3-4), 235-251.
- Faulkner, D., Rutter, E., 2001. Can the maintenance of overpressured fluids in large strike-slip fault zones explain their apparent weakness? *Geology*, 29(6), 503-506.

- Faulkner, D.R., Jackson, C.A.L., Lunn, R.J., Schlische, R.W., Shipton, Z.K., Wibberley, C.A.J., Withjack, M.O., 2010. A review of recent developments concerning the structure, mechanics and fluid flow properties of fault zones. *Journal of Structural Geology*, 32(11), 1557-1575.
- Flint, A., Flint, L., Kwicklis, E., Bodvarsson, G., Fabryka-Martin, J., 2001. Hydrology of Yucca Mountain, Nevada. *Reviews of Geophysics*, 39(4), 447-470.
- Folch, A., Mas-Pla, J., 2008. Hydrogeological interactions between fault zones and alluvial aquifers in regional flow systems. *Hydrological Processes*, 22(17), 3476-3487.
- Font-Capó, J., Vazquez-Suné, E., Carrera, J.; Martí, D.; Carbonell, R., Perez-Estaun, A., 2011. Groundwater inflow prediction in urban tunneling with a tunnel boring machine (TBM). *Engineering Geology*, 121(1-2), 46-54.
- Forster, C., Evans, J., 1991. Hydrogeology of thrust faults and crystalline thrust sheets - results of combined field and modeling studies. *Geophysical Research Letters*, 18(5), 979-982.
- Gleeson, T., Novakowski, K., 2009. Identifying watershed-scale barriers to groundwater flow: lineaments in the Canadian shield. *Geological Society of America Bulletin*, 121(3-4), 333-347.
- Goddard, J., Evans, J., 1995. Chemical-changes and fluid-rock interaction in faults of crystalline thrust sheets, northwestern Wyoming, USA. *Journal of Structural Geology*, 17(4), 533-547.
- Grupo de Hidrología Subterránea (GHS), 2003. Visual Transin Code. GHS—Universitat Politècnica de Catalunya. Accessed July 2006: <http://www.h2ogeo.upc.es>.
- Gudmundsson, A., 2000. Fracture dimensions, displacements and fluid transport. *Journal of Structural Geology*, 22(9), 1221-1231.
- Guimera, J., Vives, L., Carrera, J., 1995. A discussion of scale effects on hydraulic conductivity at a granitic site (el Berrocal, Spain). *Geophysical Research Letters*, 22(11), 1449-1452.
- Hsieh, P., 1998. Scale effects in fluid flow through fractured geological media, scale dependence and scale invariance in hydrology. Cambridge, United Kingdom, Cambridge University Press, p. 335-353. press.
- Illman, W.A., Neuman, S., 2001. Type curve interpretation of a cross-hole pneumatic injection test in unsaturated fractured tuff. *Water Resources Research*, 37(3), 583-603.
- Illman, W.A., Neuman, S., 2003. Steady-state analysis of cross-hole pneumatic injection tests in unsaturated fractured tuff. *Journal of Hydrology*, 281(1-2), 36-54.
- Illman, W.A., Tartakovsky, D.M., 2006. Asymptotic analysis of cross-hole hydraulic tests in fractured granite. *Ground Water*, 44(4), 555-563.
- Illman, W., 2006. Strong field evidence of directional permeability scale effect in fractured rock. *Journal of Hydrology*, 319(1-4), 227-236.
- Illman, W.A., Liu, X., Takeuchi, S., Yeh, T.-C.J., Ando, K., Sae-gusa, H., 2009. Hydraulic tomography in fractured granite: Mizunami underground research site, Japan. *Water Resources Research*, 45(W01406). 1-18.
- Kim, Y., Peacock, D., Sanderson, D., 2004. Fault damage zones. *Journal of Structural Geology*, 26(3), 503-517.
- Knudby, C., Carrera, J., 2005. On the relationship between indicators of geostatistical, flow and transport connectivity. *Advances in Water Resources*, 28(4), 405-421.
- Knudby, C., Carrera, J., 2006. On the use of apparent hydraulic diffusivity as an indicator of connectivity. *Journal of Hydrology*, 329(3-4), 377-389.
- Krishnamurthy, J., Mani, A., Jayaraman, V., Manivel, M., 2000. Groundwater resources development in hardrock terrain. *International Journal of Applied Earth Observation and Geoinformation*, 2(3-4), 204-215.
- Le Borgne, T., Bour, O., Paillet, F.L., Caudal, J.P., 2006. Assessment of preferential flow path connectivity, and hydraulic properties at single-borehole and cross-borehole scales in a fractured aquifer. *Journal of Hydrology*, 328(1-2), 347-359.
- Lipponen, A., Airo, M., 2006. Linking regional-scale lineaments to local-scale fracturing and groundwater inflow into the Paijanne water-conveyance tunnel, Finland. *Near Surface Geophysics*, 4(2), 97-111.
- Lipponen, A., 2007. Applying GIS to assess the vulnerability of the Paijanne water-conveyance tunnel in Finland. *Environmental Geology*, 53(3), 493-499.
- Lunn, R.J., Willson, J.P., Shipton, Z.K., Moir, H., 2008. Simulating brittle fault growth from linkage of preexisting structures. *Journal of Geophysical Research-Solid Earth*, 113(B7403), 1-10.
- Mabee, S., 1999. Factors influencing well productivity in glaciated metamorphic rocks. *Ground Water*, 37(1), 88-97.
- Mabee, S., Curry, P., Hardcastle, K., 2002. Correlation of lineaments to ground water inflows in a bedrock tunnel. *Ground Water*, 40(1), 37-43.
- Martí, D., Carbonell, R., Flecha, I., Palomeras, I., Font-Capó, J., Vazquez-Suné, E., Perez-Estaun, A., 2008. High-resolution seismic characterization in an urban area: subway tunnel construction in Barcelona, Spain. *Geophysics*, 73(2), b41-b50.
- Martinez-Landa, L., Carrera, J., 2005. An analysis of hydraulic conductivity scale effects in granite (full-scale engineered barrier experiment (FEBEX), Grimsel, Switzerland). *Water Resources Research*, 41(W03006), 1-13.
- Martinez-Landa, L., Carrera, J., 2006. A methodology to interpret cross-hole tests in a granite block. *Journal of Hydrology*, 325(1-4), 222-240.
- Mayer, J., Sharp, J., 1998. Fracture control of regional groundwater flow in a carbonate aquifer in a semi-arid region. *Geological Society of America Bulletin*, 110(2), 269-283.
- Mayer, A., May, W., Lukkarila, C., Diehl, J., 2007. Estimation of fault-zone conductance by calibration of a regional groundwater flow model: desert hot springs, California. *Hydrogeology Journal*, 15(6), 1093-1106.
- Mcgrath, A., Davison, I., 1995. Damage zone geometry around fault tips. *Journal of Structural Geology*, 17(7), 1011-1024.
- Medina, A., Carrera, J., 1996. Coupled estimation of flow and solute transport parameters. *Water Resources Research*, 32(10), 3063-3076.

- Meier, P., Carrera, J., Sanchez-Vila, X., 1998. An evaluation of Jacob's method for the interpretation of pumping tests in heterogeneous formations. *Water Resources Research*, 34(5), 1011-1025.
- Molinero, J., Samper, J., Juanes, R., 2002. Numerical modeling of the transient hydrogeological response produced by tunnel construction in fractured bedrocks. *Engineering Geology*, 64(4), 369-386.
- Moon, J., Jeong, S., 2011. Effects of highly pervious geological features on ground-water flow into a tunnel. *Engineering Geology*, 117(3-4), 207-216.
- Perrochet, P., Dematteis, A., 2007. Modeling transient discharge into a tunnel drilled in a heterogeneous formation. *Ground Water*, 45(6), 786-790.
- RSE Aplicaciones Territoriales S.A. – Unión Temporal de Empresas Linia9 – Gestor d'Infraestructures S.A., 2003, Tram 4t (B20). Informe tècnic geològic, geotècnic i hidrogeològic del tram IV, Barcelona, 43.
- Sanchez-Vila, X., Meier, P., Carrera, J., 1999. Pumping tests in heterogeneous aquifers: an analytical study of what can be obtained from their interpretation using Jacob's method. *Water Resources Research*, 35(4), 943-952.
- Sener, E., Davraz, A., Ozcelik, M., 2005. An integration of GIS and remote sensing in groundwater investigations: a case study in Burdur, Turkey. *Hydrogeology Journal*, 13(5-6), 826-834.
- Shaban, A., El-Baz, F., Khawlie, M., 2007. The relation between water-wells productivity and lineaments morphometry: selected zones from Lebanon. *Nordic Hydrology*, 38(2), 187-201.
- Shang, Y., Xue, J., Wang, S., Yang, Z., Yang, J., 2004. A case history of tunnel boring machine jamming in an inter-layer shear zone at the Yellow river diversion project in China. *Engineering Geology*, 71(3-4), 199-211.
- Shapiro, A.M., Hsieh, P.A., 1991. Research in fractured-rock hydrogeology: characterizing fluid movement and Chemicals transport in fractured rock at the Mirror Lake drainage basin. In: Mallard, G.E., Aronson, D.A. (eds.). *Proceedings of the Technical Meeting of US Geological Survey Toxic Substances Hydrology Program*. Monterey, March 11–15, Reston, US Geological Survey, Water Resources Investigation Report, 91-4034.
- Shapiro, A., 2003. The effect of scale on the magnitude of formation properties governing fluid movement and chemical transport in fractured rock. In *Groundwater in fractured rocks*. Prague (Czech Republic), September 15–19, Proceedings of the international conference, 13-14.
- Smith, L., Schwartz, F., 1984. An analysis of the influence of fracture geometry on mass-transport in fractured media. *Water Resources Research*, 20(9), 1241-1252.
- Sultan, M., Wagdy, A., Manocha, N., Sauck, W., Gelil, K.A., Youssef, A.F., Becker, R., Milewski, A., El Alfy, Z., Jones, C., 2008. An integrated approach for identifying aquifers in transcurrent fault systems: The Najd shear system of the Arabian Nubian shield. *Journal of Hydrology*, 349(3-4), 475-488.
- Tseng, D., Tsai, B., Chang, L., 2001. A case study on ground treatment for a rock tunnel with high groundwater ingress in Taiwan. *Tunnelling and Underground Space Technology*, 16(3), 175-183.
- Yang, F.R., Lee, C.H., Kung, W.J., Yeh, H.F., 2009. The impact of tunneling construction on the hydrogeological environment of "Tseng-Wen reservoir transbasin diversion project" in Taiwan. *Engineering Geology*, 103(1-2), 39-58.
- Yang, S.Y., Yeh, H.D., 2007. A closed-form solution for a confined flow into a tunnel during progressive drilling in a multi-layer groundwater flow system. *Geophysical Research Letters*, 34(7), 1-5.
- Yechieli, Y., Kafri, U., Wollman, S., Lyakhovsky, V., Weinberger, R., 2007. On the relation between steep monoclinial flexure zones and steep hydraulic gradients. *Ground Water*, 45(5), 616-626.

Manuscript received May 2011;

revision accepted May 2011;

published Online March 2012.